# Symmetry of wurtzite nanostructures with the *c*-axis in the layer plane

P. Tronc*
*Laboratoire d'Optique Physique, Ecole Supérieure de Physique et Chimie Industrielles, 10 rue Vauquelin, 75005 Paris, France*

P. Vennéguès
*CRHEA-CNRS, rue B. Grégory, 06560 Valbonne, France*

(Received 14 February 2007; revised manuscript received 25 January 2008; published 28 February 2008)

In wurtzite-based quantum wells and superlattices with the *c*-axis parallel to the layer plane, the plane is parallel to either a symmetry plane of the wurtzite lattice (type I structures, the $\langle 11-20\rangle$ growth direction) or a glide plane parallel to the *c*-axis (type II structures, the $\langle 10-10\rangle$ growth direction). We show that, in both cases, the space symmetry of the structure depends on the parity of the number of monolayers within the slab(s). The point symmetry is $C_{2v}$ except for the type II structures with odd number(s) of monolayers. The latter structures have the $\sigma_v$ point symmetry and can present a built-in electric field. Quite different selection rules, depending on the structure symmetry, govern electron optical transitions and exciton radiative recombination as well as first- and second-order infrared absorption. The intensities of the various dipolar, infrared, and Raman lines are discussed. The effect of applied magnetic and electric fields is presented. A simple optical test is proposed to distinguish the structures with the $\sigma_v$ point symmetry and those with the $C_{2v}$ one.

DOI: 10.1103/PhysRevB.77.075336 PACS number(s): 78.67.−n, 61.46.−w

## I. INTRODUCTION

The wurtzite lattice is a polar one. The nanostructures grown along the *c*-axis direction present a huge built-in electric field arising from the piezoelectric effect and the difference in spontaneous polarizability between the well and barrier materials. The field reduces the electron and hole eigenenergies (quantum confined Stark effect) and hence the radiative recombination energies. For wide enough wells, the ground transition can be lower in energy than the well-material band gap. In addition, the field spatially separates electrons from holes, thus reducing the exciton binding energy and the oscillator strength for radiative recombination. Such effects have been evidenced experimentally and computed numerically in numerous papers [see, for example, Refs. 1–3 for GaN-based quantum wells (QWs) and Ref. 4 for ZnO-based ones]. In order to cancel the built-in field or at least to reduce its strength, structures have been grown with the *c*-axis in the layer plane. Wurtzite heterostructures such as QWs or superlattices (SLs) can be grown with the layer plane being parallel to a symmetry plane (type I heterostructure, the $\langle 11-20\rangle$ growth direction) or to one of the three glide planes parallel to the *c*-axis (type II heterostructure, $\langle 10-10\rangle$ growth direction). The growth of wurtzite III-nitride or ZnO heterostructures along the $\langle 11-20\rangle$ direction has already been achieved using substrates such as (11−20) 6H-SiC (Ref. 5) and 4H-SiC,[6] (01−12) $LiTaO_3$,[7] or (1−102) sapphire.[8] (100) $\gamma$-$LiAlO_2$,[9] (10−10) 6H-SiC,[10] or even (10−10) GaN (Ref. 11) have been used to obtain growth along $\langle 10-10\rangle$.

We study hereafter the consequences of the various symmetries of the nanostructures on their electronic, optical, and vibrational properties. The present paper is organized as follows. Section II is devoted to space-symmetry analysis of QWs and SLs, site symmetry of atoms in the lattice, and symmetry reduction by an applied magnetic or electric field. In the following section, the selection rules for dipolar optical transitions, exciton radiative recombination, infrared absorption, and Raman scattering are established together with the relative strengths of their various lines. In Sec. IV, it is shown that a piezoelectric field is forbidden from symmetry in most of the structures, except those with an odd number of monolayers within the slab(s). In the latter structures, piezoelectric field can exist but should be weak. Some experiments are suggested to distinguish structures with the $\sigma_v$ and $C_{2v}$ point symmetries, respectively. Finally, Sec. V provides a brief summary of the results.

## II. SYMMETRY ANALYSIS

The wurtzite lattice ($C_{6v}^4$ nonsymmorphic space group) has a threefold rotation axis and a $6_3$ improper rotation (screw) axis. Both axes are parallel to the *c* direction but do not coincide one with the other. In addition, the $6_3$ screw axis is also a threefold rotation axis. Whereas atoms of the lattice lie on the threefold axes, the $6_3$ axes do not bear atoms. The three symmetry planes are parallel to the *c*-axis and each of the three glide planes parallel to the *c*-axis is perpendicular to one of the symmetry planes (Fig. 1). Hereafter, we consider heterostructures whose well and barrier materials are stoichiometric binary compounds with common anion or cation as, for example, $(GaN)_m/AlN$ QWs or $(GaN)_m(AlN)_n$ SLs (ZnO-based structures have also been grown). Whereas the monolayers are regularly spaced in type I heterostructures, they form closely spaced pairs in type II heterostructures (Fig. 1).

When analyzing the QW and SL structures, we adopt the approximation that the atoms are on the sites of a wurtzite lattice with lattice constants being averages between the lattice parameters of well and barrier materials. Taking this approximation into account, the coordinates of all the atoms in the lattice are well defined, and one can determine both the space group and the atomic arrangement over the Wyckoff positions for arbitrary numbers of monolayers *m* and *n*. The

 

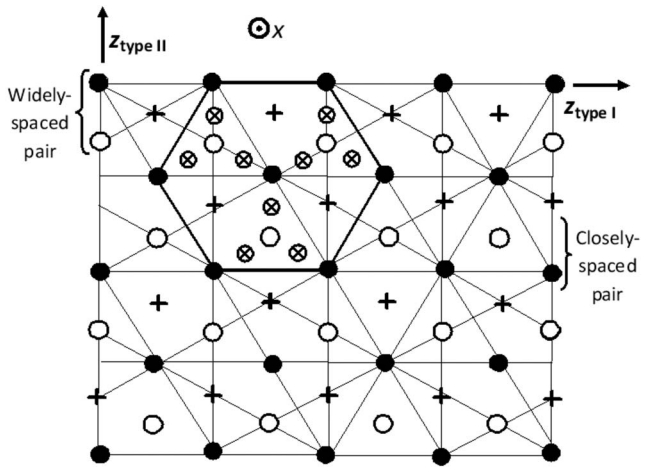


FIG. 1. Structure of $AB$ wurtzite lattice with the $c$-axis ($x$ axis) perpendicular to the sheet. Black dot: $A$ (or $B$) site within the $x=0$ plane. Open dot: site with an atom of the same species as within the $x=0$ plane but located within the first adjacent layer. Atoms of the other species are not shown. Each atomic site is located on a threefold rotation axis perpendicular to the $x=0$ plane. Cross: location of a $6_3$ screw axis perpendicular to the $x=0$ plane. Crossed dot: location (restricted to an hexagon) of a $2_1$ screw axis perpendicular to the $x=0$ plane. The $z$ axes for type I and type II structures are indicated.

space symmetry of QWs is described by layer groups (hereafter, the labeling of layer groups follows Ref. 12), whereas that of SLs is described by space groups. In our notation, the $x$ axis coincides with the $c$-axis of the wurtzite lattice and the $z$ direction is perpendicular to the layer plane. Each layer group has the same symmetry operations, except the translations along the $z$ axis, as one particular three-dimensional three-periodic space group that will be labeled hereafter as the corresponding group.[13] The correspondence between layer groups and three-dimensional three-periodic space groups is provided in Ref. 14. The two-dimensional Brillouin Zone (BZ) of the layer group coincides with the $(k_x,k_y)$ restriction of the BZ of the corresponding three-dimensional three-periodic space group and presents the same symmetry properties as the restriction. In particular, the layer group and its corresponding group have the same point symmetry. The irreducible representations (IRs) of the little group of the $(k_x,k_y)$ wave vector can be taken directly from the tables of the IRs of the corresponding three-dimensional three-periodic space group. The optical selection rules can be established using the conventional procedure. In particular, the $(k_x,k_y)$ wave vector has to be kept in a direct transition. Within the two-dimensional BZ, the optical selection rules are the same as for the corresponding space group in the $(k_x,k_y)$ plane.

(1) Except the type II QWs with odd values of $m$, the lattice of any QW is a primitive orthorhombic/rectangular and presents a $2_1$ screw axis parallel to the $x$ axis (Fig. 1). In addition, one has the following symmetry elements.

In type I QWs, there is a glide plane parallel to $(x,z)$ with improper translation parallel to $x$. For even values of $m$, there is also a glide plane parallel to $(x,y)$ with improper translation parallel to $y$, the layer group being $L33$ ($pb2_1a$) and the corresponding group $C_{2v}^5$ and for odd values of $m$, a symmetry plane parallel to $(x,y)$, the layer group being $L29$ ($pb2_1m$) and the corresponding group $C_{2v}^2$.

The structure of type II QWs with even values of $m$ is made of either closely spaced pairs of monolayers only or widely spaced pairs of monolayers only (Fig. 1). In both cases, there is a symmetry plane parallel to $(x,z)$ and a glide plane parallel to $(x,y)$. In the former case, the improper translation is diagonal for $m=2$ $(2M-1)$ and parallel to $x$ for $m=4N$, where $M$ and $N$ are positive integers (for example, for $m=2$, the improper translation is diagonal). In the latter case, the direction of the improper translation for a given value of $m$ is exchanged in comparison with that occurring in the former case. The layer group and corresponding group are $L28$ ($pm2_1b$) and $C_{2v}^2$, respectively, when the improper translation is parallel to $x$ and $L32$ ($pm2_1n$) and $C_{2v}^7$, respectively, when it is diagonal.

For type II QWs with odd values of $m$, the lattice is monoclinic/rectangular, and the only symmetry element is a symmetry plane parallel to $(x,z)$. The layer group is $L11$ ($pm11$) and the corresponding group is $C_s^1$.

(2) The symmetry of SLs includes the translational symmetry along the $z$ direction. It implies that the SL period involves an integer number of the wurtzite-lattice period in the growth direction. Therefore, $m+n$ should be equal to $2P$ and $4Q$ for type I and type II SLs, respectively, where $P$ and $Q$ are positive integers. It follows that $m$ and $n$ should have the same parity. There is no other limitation for type I SLs. For type II SLs, the pairs of $(m,n)$ values [for example, (2,4) or (3,3)] that are not such that $m+n$ is an integer multiple of 4 are forbidden since they preclude the SL translational symmetry along the $z$ direction. The SL symmetry is described by space groups. The type II SLs with odd values of $m$ and $n$ have only a single point symmetry element, i.e., a symmetry plane parallel to $(x,z)$. Their space symmetry is described by the $C_s^1$ space group. For other SLs, there is a $2_1$ screw axis parallel to the $x$ axis (Fig. 1). In addition, one has the following symmetry elements.

In type I SLs, there is a glide plane parallel to $(x,z)$ with improper translation parallel to $x$. For even values of $m$ and $n$, there is also a glide plane parallel to $(x,y)$ with improper translation parallel to $y$, the space group being $C_{2v}^5$, and for odd values of $m$ and $n$, a symmetry plane parallel to $(x,y)$, the space group being $C_{2v}^2$.

The structure of type II SLs with even values of $m$ and $n$ is made of either only closely spaced pairs of monolayers or only widely spaced pairs of monolayers (Fig. 1). In both cases, there are a symmetry plane parallel to $(x,z)$ and a glide plane parallel to $(x,y)$. In the former case, the direction of the improper translation can be deduced from those in single QWs with the same numbers of monolayers as in the SL well and barrier slabs using the following relations:

$$\text{(diagonal)} \times \text{(diagonal)} \rightarrow \text{(diagonal)},$$

$$(\|x) \times (\|x) \rightarrow (\|x), \tag{1}$$

where the direction of the SL improper translation appears in the right side of the relations. For example, for $m=n=2$, the

TABLE I. Space symmetries of the various structures.

| | Space symmetry | Corresponding group |
|---|---|---|
| | QW | |
| Type I even $m$ | $L33$ $(pb2_1a)$ | $C_{2v}^5$ $(Pca2_1)$ |
| odd $m$ | $L29$ $(pb2_1m)$ | $C_{2v}^2$ $(Pmc2_1)$ |
| Type II even $m$ (see text) | $L28$ $(pm2_1b)$ | $C_{2v}^2$ $(Pmc2_1)$ |
| | or $L32$ $(pm2_1n)$ | $C_{2v}^7$ $(Pmn2_1)$ |
| odd $m$ | $L11$ $(pm11)$ | $C_s^1$ $(P1m1)$ |
| | SL | |
| Type I $(m+n=2P)$ even $m$ and $n$ | $C_{2v}^5$ $(Pca2_1)$ | |
| odd $m$ and $n$ | $C_{2v}^2$ $(Pmc2_1)$ | |
| Type II $(m+n=4Q)$ even $m$ and $n$ (see text) | $C_{2v}^2$ $(Pmc2_1)$ | |
| | or $C_{2v}^7$ $(Pmn2_1)$ | |
| odd $m$ and $n$ | $C_s^1$ $(P1m1)$ | |

improper translation is diagonal. Note that the well and barrier slabs cannot have different improper-translation directions. Indeed, $m+n$ would be $[4(M+N)-2]$ that cannot be equal to $4Q$. Relations (1) also hold in the latter case.

The SLs with the improper translation parallel to $x$ have the $C_{2v}^2$ space group, whereas those with the diagonal translation have the $C_{2v}^7$ group.

The results concerning both QWs and SLs are displayed in Table I. It is noteworthy that the $2_1$ screw axis of the structures with the $C_{2v}$ point symmetry is, in any case, parallel to the $c$-axis of the wurtzite lattice.

(3) The site symmetry of an atom in the lattice is $C_1$ (no symmetry), except when the atom is located within a symmetry plane. In the latter case, the site symmetry includes the plane and is described by the $C_s$ group (the $\sigma_v$ or $\sigma_h$ group depending the symmetry plane is perpendicular or parallel to the layer plane).

(4) A uniform magnetic field (axial vector) applied to a structure keeps a symmetry or glide plane (the latter with its improper translation) when perpendicular to it.[15] The field also keeps any translation, as well as those rotations whose axes are parallel to its direction. For example, the $2_1$ screw axis of the structures with the $C_{2v}$ point symmetry is kept when the field is parallel to it. In addition, the gauge transformations under the symmetry operations strongly modify the symmetry properties of the electron wave functions.[15] In two-periodic structures, the Hamiltonian symmetry is described by a rod group when the field lies in the layer plane and by a point group when it does not. In three-periodic structures such as SLs, for example, the symmetry is described by a rod group whose axis is parallel to the field.

An electric field keeps a symmetry plane when contained within it. For a glide plane to be kept by the electric field, the latter has to be in the plane and perpendicular to the improper translation. An electric field lifts the translational symmetry in the directions that are not perpendicular to it. The space symmetry of a SL reduces to a two-dimensional group whose plane is perpendicular to the field. That of a QW reduces to a rod group whose direction is perpendicular to the field except in the case when the field is perpendicular to the layer plane. In the latter case, the space symmetry is described by a two-dimensional group.

## III. DIPOLAR OPTICAL SELECTION RULES, EXCITON RADIATIVE RECOMBINATION, INFRARED ABSORPTION, AND RAMAN SCATTERING

Bulk hexagonal GaN and ZnO are direct-gap semiconductors (at the $\Gamma$ point). The symmetries of the lower conduction band and of the three upper valence bands (the latter in increasing order of energy) in GaN are described by the $\Gamma_7$, $\Gamma_9$, $\Gamma_7$, and $\Gamma_7$ double-valued IRs of the $C_{6v}^4$ space group, respectively. Hereafter, the labeling of space group IRs follows Ref. 16. Note that when the spin-orbit interaction (SOI) is not taken into account, the symmetries of the lower conduction band and of the upper valence bands (they are only two) are described by the $\Gamma_1$, $\Gamma_6$, and $\Gamma_1$ single-valued IRs of the $C_{6v}^4$ space group, respectively.[17] With the account of SOI, the $\Gamma_1$ IR transforms into $\Gamma_7$, whereas $\Gamma_6$ splits into $\Gamma_7+\Gamma_9$. In ZnO, the symmetries of the lower conduction band and of the three upper valence bands are the same as in GaN, but the ordering in energy of the valence bands is perhaps different. It seems reasonable to assume that the nanostructures considered in the present paper are, such as bulk GaN and ZnO, direct-gap semiconductors at the $\Gamma$ point, except perhaps for structures with very thin slabs (few monolayers) as occurs for some GaAs/AlAs SLs with the zinc blende lattice. For this reason, our study is focused onto the $\Gamma$ point for dipolar optical electron transitions.

### A. Dipolar optical selection rules

The symmetry of the various structures allows the following conclusions concerning their optical properties to be drawn.

TABLE II. Kronecker products of (a) Γ double-valued IRs and (b) Γ single-valued IRs in the structures with the $\sigma_v$ point group and polarizations in parentheses for the allowed transitions.

| (a) | | $\Gamma_3$ | $\Gamma_4$ |
|---|---|---|---|
| | $\Gamma_3$ | $\Gamma_1(x,y)$ | $\Gamma_2(y)$ |
| | $\Gamma_4$ | $\Gamma_2(y)$ | $\Gamma_1(x,z)$ |
| (b) | | $\Gamma_1$ | $\Gamma_2$ |
| | $\Gamma_1$ | $\Gamma_1(x,z)$ | $\Gamma_2(y)$ |
| | $\Gamma_2$ | $\Gamma_2(y)$ | $\Gamma_1(x,z)$ |

(1) The QWs with the $L11$ space symmetry and the SLs with the $C_s^1$ space symmetry have the $\sigma_v$ symmetry for the Γ point. The subduction procedure of the relevant Γ IRs of the $C_{6v}^4$ group onto its $L11$ or $C_s^1$ subgroup provides the following correspondence:

$$\text{without the account of the SOI:} \quad \Gamma_1 \to \Gamma_1, \quad \Gamma_6 \to \Gamma_1 + \Gamma_2,$$

$$\text{with the account of the SOI:} \quad \Gamma_7, \Gamma_9 \to \Gamma_3 + \Gamma_4. \quad (2)$$

The vector representation is $2\Gamma_1(x,z)+\Gamma_2(y)$. Therefore, there are bright excitons with the $\Gamma_1$ and $\Gamma_2$ symmetries. They radiatively recombine with the $x$,$z$ and $y$ polarizations, respectively. Table II(a) displays the Kronecker products of the double-valued IRs of the $\sigma_v$ group, together with the allowed polarizations in parentheses for the optical transitions. Note that the transitions between states with the same symmetry are allowed in the $x$ and $z$ polarizations, whereas transitions between states with different symmetries are allowed in the $y$ polarization.

(2) The other QWs and SLs have the $C_{2v}$ symmetry for the Γ point. The subduction procedure of the relevant Γ IRs of the $C_{6v}^4$ group onto its $L28$ (or 29, or 32, or 33) or $C_{2v}^2$ (or $C_{2v}^5$, or $C_{2v}^7$) subgroup provides the following correspondence:

$$\text{without the account of the SOI:} \quad \Gamma_1 \to \Gamma_1, \quad \Gamma_6 \to \Gamma_3 + \Gamma_4,$$

$$\text{with the account of the SOI:} \quad \Gamma_7, \Gamma_9 \to \Gamma_5. \quad (3)$$

In the subgroups, there is only a single double-valued IR, the $\Gamma_5$ one. Due to our choice of coordinate axes with the $z$ axis parallel to the growth direction, which is the choice usually made by experimentalists, the vector representation is $\Gamma_1(x)+\Gamma_3(y)+\Gamma_4(z)$ for the type I structures with the $C_{2v}^2$ space or corresponding group. It is $\Gamma_1(x)+\Gamma_3(z)+\Gamma_4(y)$ for the other structures with the $C_{2v}$ point symmetry. Indeed, one has to exchange $y$ and $z$ when going from the former structures to the latter ones. Keeping this in mind, results will be presented only for the type I structures with the $C_{2v}^2$ group: There is a dark exciton with the $\Gamma_2$ symmetry and bright excitons with the $\Gamma_1$, $\Gamma_3$, and $\Gamma_4$ symmetries that can radiatively recombine with the $x$, $y$, and $z$ polarizations, respectively. Relation (4) shows that any carrier transition is allowed in any polarization:

$$\Gamma_5 \times \Gamma_5 = \Gamma_1 + \Gamma_2 + \Gamma_3 + \Gamma_4. \quad (4)$$

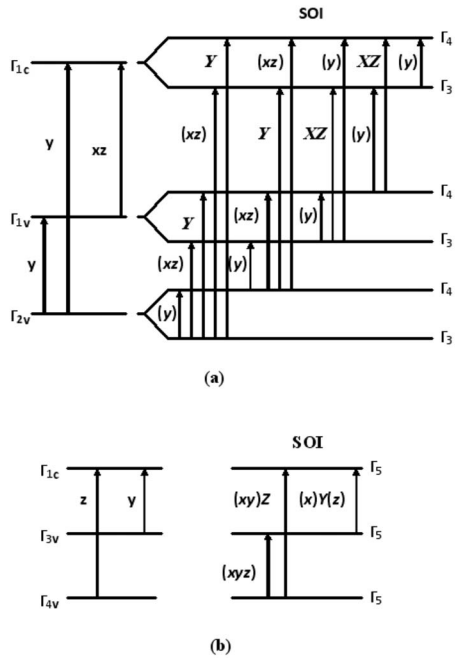


FIG. 2. Band diagram at the BZ center and polarizations for allowed dipolar optical transitions in (a) the structures with the $\sigma_v$ point symmetry and (b) the type I structures with the $C_{2v}^2$ space symmetry (for the other structures with the $C_{2v}$ point symmetry, one has to exchange $y$ and $z$). On the right side of the figure, the polarizations shown in capitals (strong transitions) are allowed both without and with the account of the SOI. The polarizations allowed only from the SOI (weak transitions) are shown in parentheses.

(3) One can be concerned about the strength of the above dipolar transitions. It is possible to find criteria for strong and weak transitions. Indeed, the strong transitions should be allowed even when the SOI is not taken into account, whereas the weak transitions should be allowed only from the SOI.

(i) For structures with the $\sigma_v$ point symmetry, the single-valued IRs transform as follows with the account of the SOI:

$$\Gamma_1, \Gamma_2 \to \Gamma_3 + \Gamma_4. \quad (5)$$

Tables II(a) and II(b) allow Fig. 2(a) to be drawn and provide the optical selection rules when the SOI is not taken into account and when it is. In the latter case, the weak transitions (i.e., the transitions allowed from the SOI only) are given in parentheses.

(ii) For structures with the $C_{2v}^2$ space symmetry, the single-valued IRs transform as follows with the account of SOI:

$$\Gamma_1, \Gamma_2, \Gamma_3, \Gamma_4 \to \Gamma_5. \quad (6)$$

Table III and relation (4) allow Fig. 2(b) to be drawn and provide the optical selection rules when the SOI is not taken into account and when it is. In the latter case, the weak transitions are given in parentheses.

The above results arise from the symmetry of the wurtzite lattice and do not depend on the binary material under consideration. Of course, some differences in oscillator strength could exist between various materials.

TABLE III. Kronecker products of the Γ single-valued IRs in the type I structures having the $C_{2v}^2$ space or corresponding group. The polarizations for infrared transitions are indicated in parentheses. The rules for the other structures with the $C_{2v}$ point group are obtained by exchanging $y$ and $z$.

| | $\Gamma_1$ | $\Gamma_2$ | $\Gamma_3$ | $\Gamma_4$ |
|---|---|---|---|---|
| $\Gamma_1$ | $\Gamma_1(x)$ | $\Gamma_2$ | $\Gamma_3(y)$ | $\Gamma_4(z)$ |
| $\Gamma_2$ | $\Gamma_2$ | $\Gamma_1(x)$ | $\Gamma_4(z)$ | $\Gamma_3(y)$ |
| $\Gamma_3$ | $\Gamma_3(y)$ | $\Gamma_4(z)$ | $\Gamma_1(x)$ | $\Gamma_2$ |
| $\Gamma_4$ | $\Gamma_4(z)$ | $\Gamma_3(y)$ | $\Gamma_2$ | $\Gamma_1(x)$ |

### B. Infrared absorption and Raman scattering

(1) In the structures with the $\sigma_v$ point group, the vector representation is $2\Gamma_1(x,z)+\Gamma_2(y)$, and the $\Gamma_1$ and $\Gamma_2$ phonon modes are infrared active in the $x$, $z$, and $y$ polarizations, respectively.

In the structures with the $C_{2v}^2$ space or corresponding group, the vector representation is $\Gamma_1(x)+\Gamma_3(y)+\Gamma_4(z)$, and the $\Gamma_1$, $\Gamma_3$, and $\Gamma_4$ phonon modes are infrared active in the $x$, $y$, and $z$ polarizations, respectively.

(2) The Raman operator is $4\Gamma_1+2\Gamma_2$ and $3\Gamma_1+\Gamma_2+\Gamma_3+\Gamma_4$ in the structures with the $\sigma_v$ and $C_{2v}$ point group, respectively. In the structures with the $\sigma_v$ point group, the $\Gamma_1$ and $\Gamma_2$ phonon modes are Raman active in the $xx$, $yy$, $zz$, and $xz$ and in the $xy$ and $yz$ polarizations, respectively. In the structures corresponding to the $C_{2v}^2$ group, the $\Gamma_1$, $\Gamma_2$, $\Gamma_3$, and $\Gamma_4$ phonon modes are Raman active in the $xx$, $yy$, and $zz$, in the $zy$, in the $yx$, and in the $xz$ polarizations, respectively. For second-order infrared absorption and Raman scattering, Table IV provides the selection rules arising from the products of phonons at high-symmetry points of the BZ for the structures with the $\sigma_v$ point group. For the structures with the $C_{2v}$ point group, Table V provides the selection rules arising from the products of phonons at the Γ point. It can be seen that the Γ phonons can induce infrared transitions with any polarization as well as Raman scattering between any pair of polarizations. Of course, some other points in the BZ should enhance the intensities of the transitions. For example, in the structures with the $C_{2v}^2$ space symmetry, the $X$, $Y$, and $S$ points in the BZ induce the same selection rules as does the Γ point.

(3) One can also be concerned about the strength of the various infrared and Raman transitions. The phonon density of states (DOS) influences the intensities of lines in the spectra. In both types of structure under study, atoms located at any Wyckoff position induce phonon modes with any possible Γ symmetry.[18] It ensures that the DOS of any type of Γ phonon is large.

TABLE IV. Second-order infrared and Raman selection rules for the structures with the $\sigma_v$ point symmetry. The Γ IRs entering into the Kronecker products of the Λ IRs are marked by a cross.

| Kronecker products ($\Lambda=\Gamma$, $A$, $B$, $C$, $D$, $E$, $Y$, or $Z$) | $\Gamma_1$ | $\Gamma_2$ | Allowed infrared polarizations | Allowed Raman polarizations |
|---|---|---|---|---|
| $\Lambda_i\times\Lambda_i$ $(i=1-2)$ | + | | $x$, $z$ | $xx$, $yy$, $zz$, $xz$ |
| $\Lambda_1\times\Lambda_2$ | | + | $y$ | $xy$, $yz$ |

TABLE V. Second-order infrared and Raman selection rules arising from the Γ phonons for the type I structures having the $C_{2v}^2$ space or corresponding group. The Γ IRs entering into the Kronecker products of the Γ IRs are marked by a cross. The rules for the other structures with the $C_{2v}$ point group are obtained by exchanging $y$ and $z$.

| | Γ part | | | | | |
|---|---|---|---|---|---|---|
| Products | $\Gamma_1$ | $\Gamma_2$ | $\Gamma_3$ | $\Gamma_4$ | Allowed infrared polarizations | Allowed Raman polarizations |
| $\Gamma_i\times\Gamma_i$ $(i=1-4)$ | + | | | | $x$ | $xx$, $yy$, $zz$ |
| $\Gamma_1\times\Gamma_2$ | | + | | | Forbidden | $yz$ |
| $\Gamma_1\times\Gamma_3$ | | | + | | $y$ | $xy$ |
| $\Gamma_1\times\Gamma_4$ | | | | + | $z$ | $xz$ |
| $\Gamma_2\times\Gamma_3$ | | | | + | $z$ | $xz$ |
| $\Gamma_2\times\Gamma_4$ | | | + | | $y$ | $xy$ |
| $\Gamma_3\times\Gamma_4$ | | + | | | Forbidden | $yz$ |

#### 1. Infrared transitions

For a transition to be allowed, the Kronecker product of initial and final electron states should include IR(s) from the vector representation. When the SOI is taken into account, it occurs for any transition in the structures with the $\sigma_v$ point symmetry [Table II(a)], or with the $C_{2v}$ one, since the $\Gamma_5\times\Gamma_5$ Kronecker product is equal to $\Gamma_1+\Gamma_2+\Gamma_3+\Gamma_4$. From the Kronecker products of single-valued IRs, it can readily be seen that any infrared transition is allowed without the account of the SOI in the structures with the $\sigma_v$ point symmetry [Table II(b)]. For structures with the $C_{2v}$ point symmetry, Table III shows that various Kronecker products of single-valued IRs involve the $\Gamma_1$ or $\Gamma_3$ or $\Gamma_4$ IR. Therefore, infrared transitions (first and second orders) involving optical phonon(s) from the vector representation should be strong since they are allowed even without the account of the SOI.

#### 2. Froelich interaction

A crystal with the wurtzite structure is made of planes perpendicular to the $c$-axis with alternate anions and cations. The phonons that induce the strongest coupling between the carriers and the lattice in the present nanostructures are among those that move rigidly parallel to the $c$ axis the planes with positively and negatively charged ions. These LO phonons give rise to the Froelich interaction and are totally symmetric with respect to the little group of the corresponding $k_x$ point in the BZ of the structure (in the structures considered in the present work, the little group of the $k_x$ vector is identical to the point group of the structure). Therefore, the phonons can connect only carrier states with the same point symmetry. As a result, among the carriers created in an excited state, only those created in a state with the same point symmetry as the ground Γ state can lower their energy

TABLE VI. Possible allowed polarizations in various optical experiments for the type I structures having the $C_{2v}^2$ space or corresponding group. The rules for the other structures with the $C_{2v}$ point group are obtained by exchanging $y$ and $z$.

| Point symmetry | $\sigma_v$ | $C_{2v}$ |
|---|---|---|
| Electron dipolar transition at Γ the point | $(x, z), y$ | $(x, y, z)$ |
| Exciton radiative recombination | $(x, z), y$ | $x, y, z$ |
| IR absorption | $(x, z), y$ | $x, y, z$ |
| Raman scattering | $xx, yy, zz, xz: xy, yz$ | $xx, yy, zz: yz: xy: xz$ |
| Second-order IR absorption | $(x, z), y$ | $x, y, z$ |
| Second-order Raman scattering | $xx, yy, zz, xz: xy, yz$ | $xx, yy, zz: yz: xy: xz$ |

to that of the latter through the Froelich interaction [under the condition that one (several) phonon (s) can fit the energy difference with the ground state and the wave-vector–conservation law]. The Froelich interaction favors the formation of polarons, since the interaction energy between the carrier or exciton and the phonon is maximal in the case. Since the phonon involved in such a polaron is totally symmetric, the formation of a polaron imposes that the initial carrier and the final polaron should have the same point symmetry.

#### *3. Raman spectroscopy*

The Froelich interaction favors the coupling between electrons and phonons. As a consequence, the transitions involving the $x$ polarization should be strong. Of course, differences in atomic masses and/or deformation potentials can induce notable changes in the results when going from one material to another.

## IV. DISCUSSION

A built-in electric field arising from piezoelectric effect and/or the difference in spontaneous polarizability between the well and barrier materials can exist only in the structures with the $\sigma_v$ point symmetry [the type II structures with odd number(s) of monolayers within the slab(s)]. Indeed, the structures have neither symmetry plane nor glide plane parallel to the substrate surface. Nevertheless, the piezoelectric effect should be weak, if any, in the heterostructures since any monolayer involves the same numbers of cations and anions. Chauveau *et al.*[19] have grown by molecular beam epitaxy onto *R*-plane sapphire some *A*-plane ZnO layers 1 $\mu$m thick and two $ZnO/Zn_{0.83}Mg_{0.17}O$ QWs with well widths of 1.6 and 4.1 nm, respectively. The samples have their layer plane parallel to a symmetry plane of the wurtzite lattice (type I structures). The wells exhibit no quantum confined Stark effect, in accordance with their symmetry properties since they have the $C_{2v}$ point symmetry with a symmetry or glide plane parallel to the layers. Photoluminescence experiments on ZnO layers resolve the *A* and *B* excitons, in polarization perpendicular to the *c*-axis, and the C exciton, in polarization parallel to the *c*-axis (the notations *A*, *B*, and *C* for excitons refer to the widely used ones in bulk wurtzite materials). Therefore, only the transitions that are fully allowed i.e., those allowed even when the SOI is not taken into account,[17] appear in the spectra. Note that, when the SOI is taken into account, there exist *B* and *C* excitons with the $\Gamma_1$ and $\Gamma_6$ symmetries, respectively (in our notations, $\Gamma_5$ and $\Gamma_6$ IRs are exchanged in comparison with notations formerly used for II-VI wurtzite materials). The excitons can recombine with the polarization parallel and perpendicular to the *c*-axis, respectively, but the intensity of the transitions should be weaker since they are allowed only from the SOI.

Polarized-light experiments can help in distinguishing structures with the $\sigma_v$ point symmetry from those with the $C_{2v}$ one. Table VI displays the possible polarizations in any type of experiment for both types of structure. Raman spectroscopy (first and second orders) does not provide significant enough differences from the point of view of symmetry between structures with the $\sigma_v$ and $C_{2v}$ point groups, since in both cases activity is possible when dealing with any pair of polarizations. On the contrary, electron dipolar transitions, exciton recombination, and infrared absorption (first and second orders) obey selection rules depending on the symmetry of the structure. Application of a magnetic field in the experiments can help in efficiently distinguishing structures. For example, a magnetic field applied perpendicular to the layer plane lowers the space symmetry of the wave functions in the QWs with the $\sigma_v$ ($C_{2v}$) point group to the $C_1$ ($\sigma_h$) point symmetry (any translational symmetry is lifted since the field is perpendicular to the layer plane[15]). The optical selection rules in the structures with the $\sigma_h$ group can be deduced from those in the structures with the $\sigma_v$ one (Table II) by exchanging $y$ and $z$. On the contrary, any transition is allowed in any polarization in the $C_1$ group. It provides a simple way to distinguish the two types of structure from each other.

The parity of the well and barrier monolayer numbers should be of prime importance for the nanostructure properties when the numbers are small. For larger values, the effect should be weaker. Such a result is always assumed in the envelope function approximation that is valid for not too narrow wells and barriers and that imposes a symmetry plane parallel to the layers and located at the center of any well and barrier. Ultimately, the point symmetry of the structures becomes $C_{6v}$ when the slabs are broad enough to reach the bulk properties.

## V. CONCLUSION

We determined the space symmetries of the various wurtzite-based QWs and SLs with the *c* axis in the layer

plane. The latter is parallel to either a symmetry plane of the wurtzite structure (type I nanostructure) or a glide plane (type II nanostructure). A built-in electric field is forbidden from symmetry except in type II nanostructures with an odd number of monolayers in the well and in the barrier for SLs. The selection rules have been established both for intraband and interband dipolar optical transitions and the intensities of the various lines discussed. The selection rules for first- and second-order infrared absorption are different for structures with the $\sigma_v$ and $C_{2v}$ point symmetries, respectively. Froelich interaction takes place along the $c$-axis direction. A magnetic field applied perpendicular to the layer plane allows QWs with the $C_{2v}$ point group to be very simply distinguished from those with the $\sigma_v$ one using optical measurements.

## ACKNOWLEDGMENTS

We acknowledge Grants No. 11156RF and No. 16254YE from the Ministère des Affairs Etrangères (France) and thank Yu. Kitaev and M. Laugt for very fruitful discussions.

*tronc@optique.espci.fr

[1] Jin Seo Im, H. Kollmer, J. Off, A. Sohmer, F. Scholz, and A. Hangleiter, Phys. Rev. B **57**, R9435 (1998).
[2] N. Grandjean, B. Damilano, S. Dalmasso, M. Leroux, M. Laugt, and J. Massies, J. Appl. Phys. **86**, 3714 (1999).
[3] Mathieu Leroux, Nicolas Grandjean, Jean Massies, Bernard Gil, Pierre Lefebvre, and Pierre Bigenwald, Phys. Rev. B **60**, 1496 (1999).
[4] C. Morhain, T. Bretagnon, P. Lefebvre, X. Tang, P. Valvin, T. Guillet, B. Gil, T. Taliercio, M. Teisseire-Doninelli, B. Vinter, and C. Deparis, Phys. Rev. B **72**, 241305(R) (2005).
[5] M. D. Craven, F. Wu, A. Chakraborty, B. Imer, U. K. Mishra, S. P. DenBaars, and J. S. Speck, Appl. Phys. Lett. **84**, 1281 (2004).
[6] N. Onojima, J. Suda, T. Kimoto, and H. Matsunami, Appl. Phys. Lett. **83**, 5208 (2003).
[7] S. H. Lim and D. Shindo, J. Appl. Phys. **88**, 5107 (2000).
[8] T. Sasaki and S. Zembutsu, J. Appl. Phys. **61**, 2533 (1987); M. D. Craven, S. H. Lim, F. Wu, J. S. Speck, and S. P. DenBaars, Appl. Phys. Lett. **81**, 469 (2002).
[9] Y. Jun Sun, O. Brandt, U. Jahn, T. Yu Liu, A. Trampert, S. Croneneberg, S. Dhar, and K. H. Ploog, J. Appl. Phys. **92**, 5714 (2002).
[10] M. McLaurin, T. E. Mates, and J. S. Speck, Appl. Phys. Lett. **86**, 262104 (2005).
[11] C. Q. Chen, M. E. Gaevski, W. H. Sun, E. Kuokstis, J. P. Zhang, R. S. Q. Fareed, H. M. Wang, J. W. Yang, G. Simin, M. A. Khan, H. P. Maruska, D. W. Hill, M. C. Chou, and B. Chai, Appl. Phys. Lett. **81**, 3194 (2002).
[12] *International Tables For Crystallography*, edited by Th. Hahn (Reidel, Dordrecht, 2002), Vol. E.
[13] V. P. Smirnov, R. A. Evarestov, and A. V. Leko, Fiz. Tverd. Tela (Leningrad) **27**, 2909 (1985).
[14] E. A. Woods, Bell Syst. Tech. J. **43**, 541 (1964).
[15] P. Tronc and V. P. Smirnov, Phys. Status Solidi B **244**, 2010 (2007).
[16] S. C. Miller and W. F. Love, *Tables of Irreducible Representations of Space Groups and Corepresentations of Magnetic Space Groups* (Pruett, Boulder, 1967).
[17] P. Tronc, Yu. E. Kitaev, G. Wang, M. F. Limonov, A. G. Panfilov, and G. Neu, Phys. Status Solidi B **216**, 599 (1999); Yu. E. Kitaev and P. Tronc, Phys. Rev. B **64**, 205312 (2001).
[18] M. I. Aroyo, J. M. Perez-Mato, C. Capillas, E. Kroumova, S. Ivantchev, G. Madariaga, A. Kirov, and H. Wondratschek, Z. Kristallogr. **221**, 15 (2006).
[19] J. M. Chauveau, C. Morhain, B. Lo, B. Vinter, P. Vennegues, M. Laugt, M. Tesseire-Doninelli, and G. Neu, Appl. Phys. A: Mater. Sci. Process. **88**, 65 (2007).